How are mixed-phase clouds mixed?

Alexei Korolev[1] and Jason Milbrandt[1]

[1]Environment and Climate Change Canada

Corresponding author: Alexei Korolev (alexei.korolev@ec.gc.ca)
Environment and Climate Change Canada, Atmospheric Science and Technology Directorate,
4905 Dufferin St., Toronto, ON, M3H5T4, Canada.

Key Points

1. In mixed-phase clouds droplets and ice particles may be uniformly distributed (genuinely mixed) or spatially separated (conditionally mixed).

2. Horizontal lengths of genuine mixed-phase and single phase ice and liquid clouds present a cascade of scales from 100km down to 100m or less.

3. Mixed-phase clouds have high spatial intermittency at small scales, currently unaccounted for in weather and climate models.

Abstract

Mixed-phase clouds are recognized as significant contributors to the modulation of precipitation and radiation transfer on both regional and global scales. This study is focused on the analysis of spatial inhomogeneity of mixed-phase clouds based on an extended data set obtained from airborne in-situ observations. The lengths of continuous segments of ice, liquid, and mixed-phase clouds present a cascade of scales varying from 10^2 km down to a minimum scale of 100 m determined by the spatial resolution of measurements. It was found that the phase composition of mixed-phase clouds is highly intermittent, and the frequency of occurrence of ice, liquid, and mixed-phase regions increases with the decrease of their spatial scales. The distributions of spatial scales have well-distinguished power-law dependencies. The results obtained yield insight into the morphology of mixed-phase clouds and have important implications for improvement in representing subgrid inhomogeneity of mixed-phase clouds in weather and climate models.

Plain Language Summary

In-situ observations showed that mixed-phase cloud may exist in a form of two extremes: (a) genuinely mixed, where supercooled droplets and ice particles are uniformly distributed in a cloud volume, and (b) conditionally mixed, when ice and liquid phases are spatially separated. The objective of this study is to explore spatial scales of genuinely mixed, ice and liquid phase cloud segments. It was found that the spatial scales of genuine mixed-phase, ice and liquid phase may vary from 100km down to 100m or even smaller. The obtained results are of a great importance for improvements of subgrid presentation of mixed-phase clouds in numerical weather and climate models and interpretation remote sensing measurements.

1 Introduction

Mixed-phase clouds represent a three-phase colloidal system consisting of water vapor, ice particles, and supercooled liquid droplets. Mixed-phase clouds are ubiquitous in the troposphere, occurring at all latitudes from the polar regions to the tropics (e.g., Wang et al. 2013, D'Alessandro et al. 2019). Because of their widespread nature, mixed-phase clouds play important roles in precipitation formation, and the radiative energy balance on both regional and global scales.

One of the important characteristics of mixed-phase clouds is the level of homogeneity of mixing ice particles and liquid droplets. There are two possible extremes of mixing. The first one is when ice particles are uniformly mixed (Fig. 1a). The second one is presented by an extremely inhomogeneous mixture, when ice particles and liquid droplets are clustered in single-phase liquid or ice cloud regions with a complex morphology (Fig. 1b). The first type of mixed-phase clouds is referred to as "genuine" mixed-phase and the second type is "conditional" mixed-phase (Korolev et al. 2017).

In genuine mixed-phase clouds, ice particles and liquid droplets are interacting with each other through the molecular diffusion of water vapor. In absence of dynamic forcing genuine mixed-phase clouds are colloidally unstable due to the difference of saturation water vapor pressure over ice and liquid (Korolev and Mazin, 2003). This instability results in the growth of ice particles and evaporation of liquid droplets, which eventually leads to the glaciation of a mixed-phase cloud. Such interaction of ice particles and liquid droplets in a mixed-phase environment is recognized as a Wegener-Bergeron-Findesen (WBF) process (Wegener, 1911; Bergeron, 1935; Findeisen, 1938).

Theoretical analysis suggests that glaciation time depending on temperature, ice particle concentration, and liquid water content (LWC) may vary from few minutes to tens of minutes (Korolev and Mazin, 2003). Therefore, the WBF process is an important factor limiting the endurance of genuine mixed-phase clouds.

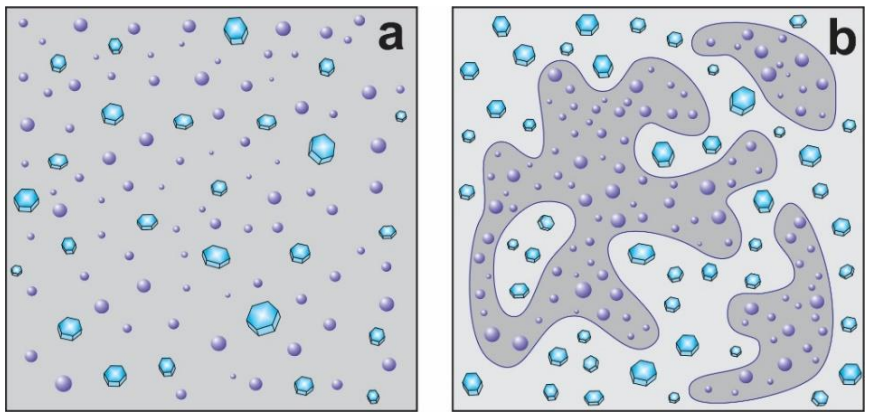

Figure 1. Conceptual diagrams of genuine (a) and conditional (b) mixed-phase clouds, representing two extremes of spatial intermittency of ice and liquid phase. The spheres and prisms denote liquid drops and ice crystals, respectively.

However, in conditional mixed-phase clouds, the interaction between ice crystals and liquid droplets is hindered because of their spatial separation in single-phase clusters (Fig. 1b). Therefore, under the assumption of supressed turbulent mixing between ice and liquid phase cloud regions, the WBF process in such clouds will be disabled, and conditional mixed-phase clouds would be colloidally stable. The endurance of such clouds is determined by processes other than the WBF mechanism. Since the WBF process enhances the growth rate of ice particles, the rate of precipitation formation in conditional mixed-phase clouds will be slower compared to that in genuine mixed-phase clouds.

Radiative properties of genuine and conditional mixed-phase clouds are also expected to be different due to the spatial clustering of ice and liquid phase (e.g. Ruiz-Donoso et al. 2020). The liquid water, initially distributed among a large number of liquid droplets, by the end of glaciation will be depleted by fewer ice particles. Therefore, the WBF process will result in a reduction of the extinction coefficient and optical thinning of genuine mixed-phase clouds. It is worth mentioning that, changes in the optical properties of mixed-phase clouds during the WBF process due to redistribution of the same amount of condensed water between a different number of scatterers is equivalent to the Twomey effect (Twomey, 1974) in liquid clouds. In contrast to the above, in conditional mixed-phase, the glaciation process is hindered, and therefore, the radiative properties will be more stable compared to the genuine mixed-phase clouds. Therefore, the net radiative effect for genuine and conditional mixed-phase clouds integrated over time will be different.

Understanding the spatial phase intermittency of clouds has great importance both for fundamental cloud physics and numerical simulations of clouds. In numerical models dealing with mixed-phase clouds, ice particles and liquid droplets are assumed to be uniformly mixed inside the grid cells with a mixed-phase environment. Depending on the type of modeling system, the horizontal grid spacing vary widely. For example, numerical weather prediction (NWP) systems use grid spacings ranging from approximately 3 to 15 km (e.g. McTaggart-Cowan et al. 2019), with some experiment systems on the hectometer scale (e.g. Joe et al. 2018), whereas global climate models run with grid spacings ranging from 60 to 300 km (Almazroui et al. 2020).The assumption about homogeneously mixed liquid droplets and ice particles may result in biases in precipitation production and radiation transfer.

In situ observations showed high spatial phase variability of clouds below the freezing temperature. Thus, Hallett (1999) observed well-separated regions of ice and liquid in sea-breeze-front clouds, where the actual mixed-phase interface was observed at the boundary separated ice and liquid regions and was only a few hundreds of meters wide. Korolev et al. (2003) showed that clusters of ice and liquid phase clouds can exist at the scale of the order of kilometers. Field et al. (2004) obtained statistics of contiguous ice, liquid, and mixed-phase cloud segments from in-situ observations in frontal clouds. They pointed out that liquid intrusion into surrounding ice clouds can be as small as 100 m. However, the maximum scale was identified as approximately 1 km. Korolev et al. (2003) hypothesized that phase intermittency may exist down to a meter, i.e., fine-scale clusters of liquid (ice) embedded in a glaciated (liquid) cloud.

This paper explores spatial phase intermittency based on a large data set of in situ cloud microphysical observations. The primary question we attempt to address in this study is: How are mixed-phase clouds mixed?

2 Methodology and the data set

The cloud phase composition was studied with a set of airborne instruments installed by Environment and Climate Change Canada (ECCC) in collaboration with the National Research Council (NRC) on the NRC Convair-580 research aircraft.

The phase composition of clouds was identified with the help of a set of instruments: Nevzorov probe (Korolev et al. 1998), Rosemount Icing Detector (Baumgardner and Rodi, 1989; Mazin et al. 2001), Forward Scattering Spectrometer Probe (FSSP) (Knollenberg, 1976, McFarquhar et al, 2017), Optical Array Probe 2DC (OAP-2DC) (Knollenberg, 1976; Baumgardner et al., 2017), and Optical Array Probe 2DP (OAP-2DP) (Knollenberg, 1976).

The Nevzorov probe was primarily used for the assessment of liquid water (LWC) and ice water content (IWC). The methodology of Nevzorov probe data processing and phase discrimination was described in detail in (Korolev et al. 1998; Korolev and Strapp, 2002). The Nevzorov probe liquid water sensor measurements were corrected on the residual effect of ice (Korolev et al. 1998, 2003; Field et al., 2004) and the total water sensor measurements were corrected on the ice bouncing effect (Korolev et al. 2013). The Rosemount Icing Detector was used to identify the presence of the liquid phase and exclude false liquid signals in ice clouds. The FSSP was employed to identify the presence of liquid droplets smaller than 45 μm in diameter. The OAP-2DC and 2DP were used for justification of the presence or absence of ice particles based on identification of non-circular shapes of their binary images.

In the present study the thresholds for liquid water content and ice water content (IWC) were set as LWC > 0.01g m^{-3}, IWC > 0.01g m^{-3}, respectively. The phase composition of clouds was identified based on the assessment of the ice water fraction $\mu = IWC/(LWC + IWC)$. Thus, clouds with $\mu > 0.9$ were considered as ice, clouds with $\mu < 0.1$ were defined as liquid, and clouds $0.1 \leq \mu \leq 0.9$ were determined as mixed-phase clouds.

The objective of the data processing was the identification of continuous ice, liquid, and mixed-phase cloud segments along the flight path of the research aircraft. Following the above definitions of clouds and cloud phase, time series of LWC and IWC were converted into three discrete cloud phase categories “ice”, “liquid” and “mixed-phase”. The processing algorithm started counting the cloud length when LWC or IWC exceeded the threshold value 0.01 g m^{-3}, and the cloud length counting was interrupted, when the cloud phase changed, or LWC and IWC became lower the

predetermined cloud water content threshold. Isolated single-phase ice or liquid clouds were defined as continuous clouds, which were not interrupted by cloud segments with another phase. Such clouds were identified and excluded from the subsequent analysis. Therefore, the ensemble of clouds used in this study is continuous cloud segments, which include both ice and liquid in a form of single-phase or mixed-phase cloud segments.

The analyzed data set includes seven flight campaigns lead by ECCC and extended over a period of ten years from 1994 to 2004: Beaufort Arctic Storm Experiment (BASE), Canadian Freezing Drizzle Experiment (phase 1 and 3) (CFDE 1 and 3), the First International Satellite Cloud Climatology Project (ISCCP) Regional Experiment Arctic Cloud Experiment (FIRE-ACE), Alliance Icing Research Study (phase 1, 1.5, 2) (AIRS 1, 1.5, 2). Table 1 presents the description of the time frames, areas of operations, number of flights, and sampled cloud lengths for each campaign.

Table 1. Summary of the flight campaigns

	project	project dates	operation base	Lat/Lon	Number of flights
1	BASE	Sep-Oct/1994	Inuvik (NT)	57°N–74°N 113°W–141°W	12
2	CFDE 1	Feb-Mar/1995	St. John's (NL)	45°N–53°N 54°W–63°W	12
3	CFDE 3	Dec/1997-Feb/1998	Ottawa (ON)	42°N–50°N 71°W–83°W	27
4	FIRE-ACE	Apr/1998	Inuvik (NT)	68°N–76°N 133°W–167°W	17
5	AIRS 1	Dec/1999-Feb/2000	Ottawa (ON)	42°N–46°N 74°W–82°W	25
6	AIRS 1.5	Feb/2003	Ottawa (ON)	42°N–46°N 74°W–82°W	8
7	AIRS 2	Nov/2003-Feb/2004	Ottawa (ON)	42°N–46°N 74°W–82°W	21

Most of the data were collected in stratiform clouds associated with mesoscale frontal systems. The altitude and temperature of the sampled clouds varied in the ranges 0.5 km < H < 7.3 km and -50°C < T < +10°C, respectively. However, in the frame of this study the measurements were limited by the temperature range -35 < T < 0C due to the low statistics of mixed and liquid clouds in the range -40°C < T < -35°C, and the absence of liquid phase at T < -40°C due to homogeneous freezing.

The entire flight operations include 117 research flights. The endurance of each flight varied from 3 h to 5 h. The total length of sampled in-cloud space extended over 55 381 km. After elimination of isolated single-phase clouds and applying temperature limitations, the total length of the clouds, which were included in the statistics, was reduced to 32 488 km.

3 Results

Figure 2 shows normalized distributions of ice, liquid and mixed-phase contiguous cloud segments in three temperature subranges -10 < T < 0°C, -20 < T < -10°C and -30 < T < -20°C. As it is seen from Fig. 2 the ice, liquid, and mixed-phase cloud regions are represented by a cascade of scales ranging from tens and hundreds of kilometers down to the minimum scale L_{min}~100 m. The minimum scale L_{min} is limited by the instrumental resolution.

The maximum scale of ice clouds ($L_{max}^{(i)}$) varies from tens kilometers at cold temperatures (-30 < T < -20°C) (Fig. 2c) to 100-300 km at T > -20°C (Figs. 2a,b). The maximum scales of liquid ($L_{max}^{(w)}$) and mixed-phase ($L_{max}^{(m)}$) cloud segments are systematically lower than $L_{max}^{(i)}$ for ice clouds. As follows from Fig. 2, $L_{max}^{(w)}$ and $L_{max}^{(m)}$ decrease from 40-60 km at -10 < T < 0°C to 10-15 km at -30 < T < -20°C. Such, relationship between L_{max} for ice and mixed-phase clouds can be explained due to the conversion of mixed-phase in ice clouds and their contribution into the spatial length of ice clouds.

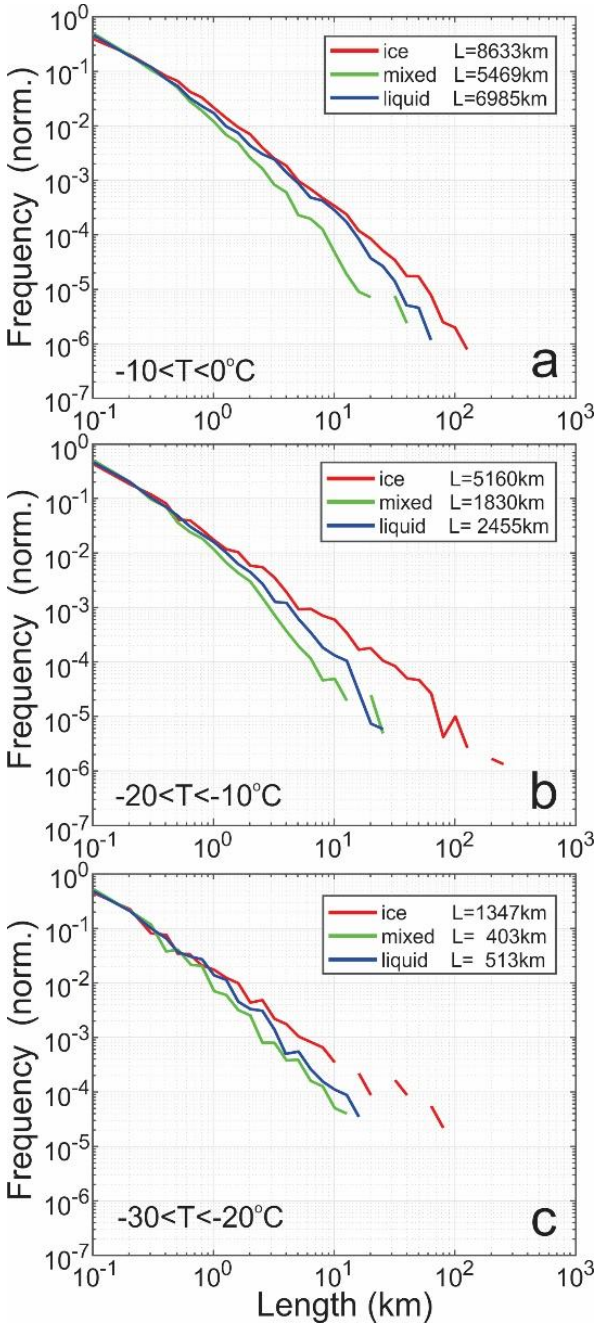

Figure 2. Distributions of continuous ice, liquid and mixed-phase cloud segments in three temperature intervals (a) -10 < T < 0°C; (b) -20 < T < -10°C; (c) -20 < T < -30°C. "L" indicates sampled cloud length.

In this study the minimum cloud phase scale L_{min} is limited by the instrumental resolution. Therefore, the mixed-phase cloud segments at scales $L \geq L_{min}$ are considered genuinely mixed down to the scale L_{min}. In fact, these clouds can be conditionally mixed at spatial scales $L < L_{min}$.

The spatial scale distributions of continuous ice, liquid and mixed-phase segments are well described by the power law $F(L) = aL^b$. The weighted least-squares fit coefficients a and b are presented in Table 2. The Pearson correlation coefficient for each parameterization in Table 2 are higher 0.99.

As it is seen from Table 2 the slope of lengths distributions for mixed-phase and liquid (Fig. 2) remains nearly constant in all temperature intervals, and it changes withing 3-4%. However, the slope of lengths distributions for ice has a clear tendency to increase toward low temperatures.

Table 2. Coefficients for the power law fitting of the normalized frequency distributions of spatial scales of ice, liquid, and mixed-phase cloud regions $F(L) = aL^b$

cloud type	-30 < T < -20°C		-20 < T < -10°C		-10 < T < 0°C	
	a	b	a	b	a	b
ice	10.5 10^{-3}	-1.44	18 10^{-3}	-1.66	17.4 10^{-3}	-1.86
mixed	7.85 10^{-3}	-2.03	8.06 10^{-3}	-2.17	8.75 10^{-3}	-2.19
liquid	24.4 10^{-3}	-1.97	11.5 10^{-3}	-2.03	13.8 10^{-3}	-1.94

Figure 3 shows temperature dependences of average continuous scales of ice, liquid, and mixed phase cloud segments. As it is seen from Fig.3 the average length of mixed-phase segments has a weak dependence on temperature and it varies between 300 m and 500 m. The mean length of liquid cloud segments is systematically larger than that of mixed-phase segments, and it gradually decreases with the decrease of temperature from approximately 1 km and 500 m. However, average lengths of continuous ice cloud segments turned out to be the largest compared to liquid and mixed-phase segments. The average length of ice cloud segments increases from 1 km at 0°C to 5 km at -25 < T < -20°C and then decrease to approximately 1 km at -35°C.

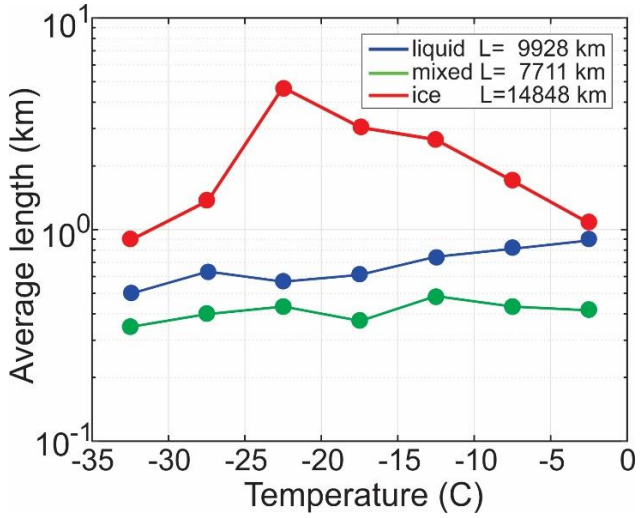

Figure 3. Average lengths of ice, liquid and mixed-phase cloud segments versus temperature.

4 Discussion

Turbulence is one of the major mechanisms mixing environments with different phases. The result of the turbulent mixing of clouds with a different phase composition is a mixed-phase cloud. The characteristic time scale (τ_t) of mixing of a cloud volume with a spatial scale L can be assessed as (Landau and Lifshitz, 1987)

$$\tau_t = \left(\frac{L^2}{\varepsilon}\right)^{1/3}, \quad (1)$$

where ε is the turbulence energy dissipation rate.

However, cloud particles are an active admixture and during mixing they are interacting with each other through water vapour. Such interaction results in activation of the WBF mechanism, if the velocity of vertical of the cloud u_z does not exceed a critical velocity u_z^* (i.e. $u_z < u_z^*$) (Korolev, 2007). The WBF process leads glaciation of the mixed phase cloud within the glaciation time (Korolev and Mazin, 2003)

$$\tau_{gl} = k\left(\frac{W}{N_i}\right)^{2/3} \quad (2)$$

Here W is the liquid water content, N_i is the concentration of ice particles; $k = \frac{\rho_i}{4\pi c S_i(T)}\left(\frac{9\pi\rho_i}{2}\right)^{1/3}\left(\frac{L_i^2}{KR_v T^2} + \frac{R_v T}{E_i(T)D}\right)$; ρ_i is the density of ice; $S_i(T) = \frac{E_w(T)}{E_i(T)} - 1$ is the supersaturation over ice at saturation pressure over water at temperature T; $E_w(T)$, $E_i(T)$ is the saturating pressure of water vapor over liquid and ice, respectively, at temperature T; R_v is the specific gas constant of water vapor; L_i is the latent heat for ice sublimation; K is the coefficient of air heat conductivity; D is the coefficient of water vapor diffusion in the air.

Thus, turbulent mixing and glaciation are two processes working in opposite directions. The turbulent mixing is tending to homogenize and maintain a mixed-phase environment. Whereas the glaciation process tends to turn a mixed-phase cloud into an ice cloud. Therefore, a mixed-phase environment may be maintained by turbulent mixing, if the glaciation time τ_{gl} exceeds the mixing time τ_t, i.e.

$$\tau_{gl} > \tau_t \quad (3)$$

Substituting Eqs. 1 and 2 in Eq. 3 yields a threshold spatial scale,

$$L_{ph} = (k\varepsilon)^{1/2}\frac{W}{N_i} \quad (4)$$

such that mixed-phase environment can exist at scales $L < L_{ph}$ at time scales satisfying Eq. 3.

Substituting ε = 10^{-3}-10^{-4} m^2 s^{-3}, W = 0.1-1.0 g m^{-3}, N_i =10^1 - 10^2 L^{-1}, -35 < T < -5°C yields the range of spatial phase scales L_{ph}~10^1 – 10^4 m. This obtained assessment of L_{ph} remarkably consistent with the range of spatial scales covered by mixed-phase clouds in Fig. 2. However, the obtained assessment, also suggests that L_{ph} may extend down to 10 m at the small-scale end.

As it is seen from Eq. 4, the spatial scale of mixed-phase clouds depends on LWC. Therefore, it is anticipated that the frequency function $F(L)$ should be related on a frequency of occurrence of LWC ($F(W)$). Figure 4 shows a probability density functions $F(W)$ at different temperatures. As it is seen from Fig. 4 $F(W)$ increases with the decrease of LWC. Therefore, following Eq. 4 the increase of occurrence of small-scale mixed-phase clouds may be explained by the increase of occurrence of LWC with the decrease of LWC. Even though $F(W)$ has a quasi-exponential dependence, whereas $F(L)$ is described by a power-law, the behaviour of LWC generally explains the behaviour of $F(L)$.

The above simplified consideration does not account cloud processes such as riming, ice sedimentation, entrainment of out-of-cloud air. However, it allows to generally predict the behaviour and the range of spatial scales of genuinely mixed-phase clouds.

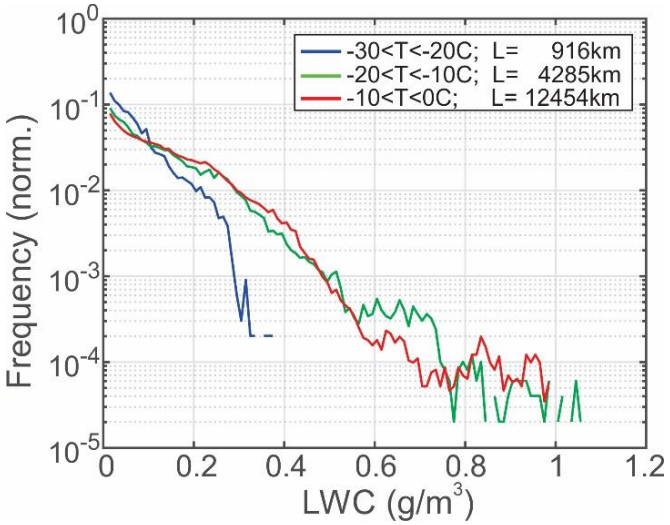

Figure 4. Normalized frequency of occurrences of LWC in liquid and mixed-phase clouds averaged over all sampled clouds. Isolated single-phase clouds were not included in these statistics.

5 Conclusions

This study presents observed spatial phase intermittency in mixed phase clouds based on a large data set collected in midlatitude and Arctic clouds. It was shown that in the temperature range -35 < T < 0°C clouds containing ice and liquid may form regions with genuinely or conditionally mixed-phase environments. The lengths of continuous segments of ice, liquid and mixed-phase cloud present a cascade of scales varying from 10^{-1}-10^{2}km down to a minimum scale L_{min}~100 m determined by the spatial resolution of the measurements. It is hypothesized that L_{min} of the genuine conditionally mixed-phase cloud regions may go down to scale of 1 -10 m. The frequency of occurrence of continuous lengths of ice, liquid and mixed-phase segments is well described by a power law (Fig. 2, Table 2).

The results obtained yield insight on the spatial morphology of mixed-phase clouds. These results also suggest a new potential direction for improvement of simulations of mixed-phase clouds in NWP and climate models whereby the subgrid phase inhomogeneity and conditionally mixed phase clouds is accounted for. For example, in the microphysics parameterization scheme of the model, the WBF process could be suppressed or reduced, based on the turbulent kinetic energy, by artificially reducing the evaporation rate of liquid and the deposition rate of ice. This would reduce the amount of glaciation and increase the likelihood of conditional mixed-phase clouds. While such an approach would be inherently ad hoc, it should be possible to calibrate the modified diffusional growth/decay rates such that the model reproduces the observed frequency distributions of liquid, ice, and mixed-phase cloud segments. Consequently, this should improve precipitation and radiative transfer calculations in the model. In a follow-up study, this approach will be investigated in the context of a NWP model with various horizontal grid spacings.

Acknowledgements

Special thanks for the NRC pilots for a great cooperation in data collection and for an outstanding operation of the NRC Convair-580 in heavy icing conditions. The BASE project was funded by ECCC. The CFDE project was supported by Canadian Search and Rescue, Transport Canada (TC). The FIRE-ACE project was supported by NASA. The AIRS project was supported by the US Federal Aviation Administration (FAA) and TC. Special thanks to the ECCC and NRC teams of technicians and engineers for installation, maintenance, and operations of the airborne instrumentation.

Data Availability Statement

Data supporting this research are available from https://doi.org/10.5281/zenodo.6558498.

Author Contributions:

Conceptualization: A. Korolev, J. Milbrandt
Data curation: A. Korolev
Formal analysis: A. Korolev
Methodology: A. Korolev
Project Administration: A. Korolev, J. Milbrandt
Writing – original draft: A. Korolev
Writing – review & editing: A. Korolev, J. Milbrandt

References

D'Alessandro, J. J., Diao, M. Wu, C. Liu, X. Jensen, J. B. & Stephens, B. B. (2019), Cloud Phase and Relative Humidity Distributions over the Southern Ocean in Austral Summer Based on In Situ Observations and CAM5 Simulations. *Journal of Climate*, *32*, 2781–2805, DOI: https://doi.org/10.1175/JCLI-D-18-0232.1

Almazroui, M., Saeed, S., Saeed, F. & Coauthors (2020), Projections of Precipitation and Temperature over the South Asian Countries in CMIP6. *Earth Systems and Environment*, 297–320. https://doi.org/10.1007/s41748-020-00157-7

Baumgardner, D., & Rodi, A. (1989), Laboratory and wind tunnel evaluation of the Rosemount icing detector. *Journal of Atmospheric and Oceanic Technology*, *6*, 971–979, https://doi.org/10.1175/1520-0426(1989)006%3C0971:LAWTEO%3E2.0.CO;2

Baumgardner, D., Abel, S. J., Axisa, D., Cotton, R., Crosier, J., Field, P., Gurganus, C., Heymsfield, A., Korolev, A., Krämer, M., Lawson, P., McFarquhar, G. Ulanowski, Z., & Um, J. (2017), Cloud Ice Properties: In Situ Measurement Challenges, *Meteorological Monographs*, *58*, 9.1–9.23, https://doi.org/10.1175/AMSMONOGRAPHS-D-16-0011.1

Bergeron, T., (1935), On the physics of clouds and precipitation. *Proces Verbaux de l'Association de Météorologie*, International Union of Geodesy and Geophysics, 156–178.

Findeisen, W. (1938), Kolloid-meteorologische Vorgänge bei Neiderschlags-bildung. *Meteorologiche Zeitschrift*, *55*, 121-133, https://doi.org/10.1127/metz/2015/0675

Isaac, G. A., Cober, S. G., Strapp, J. W., Korolev, A. V., Tremblay, A., & Marcotte, D. L. (2001), Recent Canadian research on aircraft in-flight icing. *Canadian Aeronautics and Space Journal*, *47*, 213–221.

Isaac, G.A., Ayers, J.K., Bailey, M., Bissonnette, L., Bernstein, B.C., Cober, S.G., Driedger, N., Evans, W.F.J., Fabry, F., Glazer, A., Gultepe, I., Hallett, J., Hudak, D., Korolev, A., Marcotte, D., Minnis, P., Murray, J., Nguyen, L., Ratvasky, T., Reehorst, A., Reid, J., Rodriguez, P., Schneider, T., Sheppard, B., Strapp, J.W., & Wolde, M. (2005), First Results from the Alliance Icing Research Study II. *AIAA 43rd Aerospace Sciences Meeting and Exhibit*, Reno, NV, 11-13 January, AIAA-2005-0858

Field, P. R., Hogan, R. J., Brown, P. R. A., Illingworth, A. J., Choularton, T. W., Kaye, P. H., Hirst, E., Greenaway, R. (2004), Simultaneous radar and aircraft observations of mixed-phase cloud at the 100 m scale. 130, 1877-1904, https://doi.org/10.1256/qj.03.102

Hallett, J. (1999), Charge generation with and without secondary ice production. in *Proceedings of 11th International Conference on atmospheric electricity*, NASA/CP-1999-209261, June, Huntsville, Alabama, USA, 355–358.

Joe, P., Belair, S., Bernier, N. B., Bouchet, V., Brook, J.R., Brunet, D., Burrows, W., Charland, J.P., Dehghan, A., Driedger, N. & Duhaime, C. (2018), The environment Canada pan and parapan American science showcase project. *Bulletin of the American Meteorological Society*, *99*(5), 921-953, https://doi.org/10.1175/BAMS-D-16-0162.1

Korolev, A. V., & Strapp, J. W. (2002), Accuracy of measurements of cloud ice water content by the Nevzorov probe. Preprints, *AIAA 40th Aerospace Science Meeting and Exhibit*, AIAA 2002-0679, Reno, NV, American Institute of Aeronautics and Astronautics, 1–8.

Korolev, A. V., & Mazin, I. P. (2003), Supersaturation of water vapor in clouds. *Journal of the Atmospheric Sciences*, *60***,** 2957–2974, https://doi.org/10.1175/1520-0469(2003)060%3C2957:SOWVIC%3E2.0.CO;2

Korolev, A. V., Strapp, J. W., Isaac, G. A., & Nevzorov, A. N. (1998), The Nevzorov airborne hot-wire LWC–TWC probe: Principle of operation and performance characteristics. *Journal of Atmospheric and Oceanic Technology*, *15***,** 1495–1510, https://doi.org/10.1175/1520-0426(1998)015%3C1495:TNAHWL%3E2.0.CO;2

Korolev, A. V., Isaac, G. A., Cober, S., Strapp, J. W., & Hallett, J. (2003), Microphysical characterization of mixed-phase clouds. *Quarterly Journal of the Royal Meteorological Society*, *129***,** 39–66, https://doi.org/10.1256/qj.01.204

Korolev, A., McFarquhar, G., Field, P. R., Franklin, C., Lawson, P., Wang, Z., Williams, E., Abel, S. J., Axisa, D., Borrmann, S., Crosier, J., Fugal, J., Krämer, M., Lohmann, U., Schlenczek, O., Schnaiter, M., & Wendisch, M. (2017), Mixed-Phase Clouds: Progress and Challenges. *Meteorological Monographs*, *58*, 5.1–5.50, https://doi.org/10.1175/AMSMONOGRAPHS-D-17-0001.1

Knollenberg, R. G. (1976), Three new instruments for cloud physics measurements: The 2D-spectrometer probe, the forward scattering spectrometer probe and the active scattering spectrometer probe. *Preprints, Int. Conf. on Cloud Physics*, Boulder, CO, Amer. Meteor. Soc., 554–561.

Korolev, A.V., Strapp, J. W., Isaac, G. A., & Emery, E. (2013), Improved airborne hot-wire measurements of ice water content in clouds. *Journal of Atmospheric and Oceanic Technology*, *30*, 2121-2131, https://doi.org/10.1175/JTECH-D-13-00007.1

Landau L.D., & Lifshitz E.M. (1987), *Fluid Mechanics*, Volume 6, Pergamon Press, 539 p.

Mazin, I. P., Korolev, A. V., Heymsfield, A., Isaac, G. A., & Cober, S. G. (2001), Thermodynamics of icing cylinder for measurements of liquid water content in supercooled clouds. *Journal of Atmospheric and Oceanic Technology*, *18*, 543–558, https://doi.org/10.1175/1520-0426(2001)018%3C0543:TOICFM%3E2.0.CO;2

McFarquhar, G.M., Baumgardner, D., Bansemer, A., Abel, S. J., Crosier, J., French, J., Rosenberg, P., Korolev, A., Schwarzoenboeck, A., Leroy, D., Um, J., Wu, W., Heymsfield, A. J., Twohy, C., Detwiler, A., Field, P., Neumann, A., Cotton, R., Axisa, D. & Dong, J. (2017), Processing of Ice Cloud In-Situ Data Collected by Bulk Water, Scattering, and Imaging Probes: Fundamentals, Uncertainties and Efforts towards Consistency. *Meteorological Monographs, 58*, 11.1–11.33, https://doi.org/10.1175/AMSMONOGRAPHS-D-16-0007.1

McTaggart-Cowan, R., Vaillancourt, P.A., Zadra, A., Chamberland, S., Charron, M., Corvec, S., Milbrandt, J.A., Paquin-Ricard, D., Patoine, A., Roch, M. & Separovic, L. (2019), Modernization of atmospheric physics parameterization in Canadian NWP. *Journal of Advances in Modeling Earth Systems*, *11*(11), pp.3593-3635.

O'Shea, S. J., T. Choularton, M. Flynn, K. N. Bower, M. Gallagher, J. Crosier1, P. Williams, I. Crawford, Z. L. Fleming, C. Listowski, A. Kirchgaessner, R. S. Ladkin, & T. Lachlan-Cope, (2017), In situ measurements of cloud microphysics and aerosol over coastal Antarctica during the MAC campaign. *Atmospheric Chemistry and Physics*, *17*, 13049–13070, https://doi.org/10.5194/acp-17-13049-2017

Ruiz-Donoso, E., Ehrlich, A., Schäfer, M., Jäkel1, E., Schemann, V., Crewell, S., Mech, M., Kulla, B. S., Kliesch, L.-L., Neuber, R., & Wendisch, M. (2020), Small-scale structure of thermodynamic phase in Arctic mixed-phase clouds observed by airborne remote sensing during a cold air outbreak and a warm air advection event. *Atmospheric Chemistry and Physics*, *20*, 5487–5511, https://doi.org/10.5194/acp-20-5487-2020.

Twomey, S., 1974: Pollution and the planetary albedo. *Atmos. Environ*. **8** (12): 1251–1256, doi:10.1016/0004-6981(74)90004-3

Wang, Z., Vane, D., Stephens, G., & Reinke, D. (2013), CloudSat Project: Level 2 combined radar and lidar cloud scenario classification product process description and interface control document. California Institute of Technology JPL, 61 pp, https://www.cloudsat.cira.colostate.edu/cloudsat-static/info/dl/2b-cldclass-lidar/2B-CLDCLASS-LIDAR_PDICD.P_R04.20120522.pdf

Wegener, A., (1911), *Thermodynamik der Atmosphäre*. Leipzig, 331p.